Surface Changes of Gold Electrodes Produced by Periodic Potential Treatments in HF Solutions

M. C. Galindo, C. L. Perdriel, M. E. Martins, and A. J. Arvia*

Instituto de Investigaciones Fisicoquimicas Teóricas y Aplicadas (INIFTA), Facultad de Ciencias Exactas, Universidad Nacional de La Plata, Casilla de Correo 16, Sucursal 4 (1900), La Plata, Argentina

Received May 27, 1987. In Final Form: September 28, 1988

The surface changes produced on Au in HF solutions by applying relatively fast periodic potentials are investigated. The range of frequency and potential limits can be adjusted to produce principally either transient activation for the hydrogen electrode reaction (HER) or electrochemical faceting. The first effect is largely independent of the second one, as it implies the development of a transient surface structure which facilitates hydrogen adsorption and absorption. Electrochemical faceting caused by oxidation–reduction cycles (ORC) depends on the potential limits which are associated with either Au electrodissolution and electrodeposition or Au oxide electroformation and electroreduction. Electrochemical faceting can be clearly seen through SEM micrographs, and the type of preferred orientation can be tentatively inferred from voltammetry of underpotential deposition (upd) of Pb in 10^{-3} M $Pb(ClO_4)_2$ + 1 M $HClO_4$ solution through a direct comparison with data reported in the literature for the reaction on single-crystal Au surfaces. Electrochemical faceting implies a simultaneous increase in surface roughness, as followed from changes in voltammetric charges for both upd Pb and O atom electrodesorption in acid solutions.

Introduction

The voltammetric response of polycrystalline Au in acid solutions is extremely sensitive to the history of the experiment, particularly when the electrode is subjected to a periodic potential either at low (1 mV/s) or high (10^3 V/s) potential sweep rates.[1-6] It also depends on the electrolyte composition and temperature.[7-11] The application of a periodic perturbing potential to Au in acid usually results in changes of the Au surface topography (electrochemical faceting) as well as in the electrocatalytic properties of the modified metal surface. The latter can be seen through the O electroadsorption/electrodesorption voltammogram. The electrochemical faceting of Au electrodes through square wave potential cycling at frequencies greater than 1 kHz[1,3] develops surfaces which are relatively more stable and reproducible from the standpoint of voltammetry than those obtained by either mechanical polishing, chemical etching, or electropolishing. The electrochemical faceting of Au, in contrast to Pt,[12,13] is accompanied by changes in both the real electrode surface area and the activity of the electrode for the HER.[14-21]

The present paper refers to surface modifications of Au electrodes produced by different periodic perturbing potentials in aqueous HF solutions, where anion adsorption effects are minimized. Two types of surface modifications are described, one which principally produces a remarkable activation in the HER, with relatively minor voltammetric changes in the O electroadsorption/electrodesorption potential range, and another one which causes remarkable changes in the distribution of crystallographic faces including surface defects. The latter can be followed through SEM micrographs and voltammetric O electroadsorption/electrodesorption and Pb underpotential deposition (upd)/stripping. The voltammograms for the latter reaction, run, for instance, in 10^{-3} M PbF_2 + 10^{-2} M $HClO_4$, depend on the crystallographic structure of the Au electrode surface, as it has been thoroughly investigated on Au single-crystal electrodes.[22,23] Accordingly, these data have been used in the present work as reference systems for a tentative characterization of the type of preferred crystallographic orientation resulting for electrochemically faceted Au electrodes. In the absence of a technique providing molecular level results such as in situ scanning tunneling microscopy, which is still in the early stages of development,[24] the direct voltammetric comparison in the same conditions, based on the recently reported data[22,23] appears to be a reasonable although relative way for estimating in situ the type of average topography prevailing at the treated Au electrode surfaces.

Experimental Section

Electrochemical Faceting Procedure. Runs were carried out in a Teflon electrochemical cell by using 1 and 4 M HF solutions. The working electrode consisted of small Au spheres of about 0.1-cm diameter obtained by melting the extreme of a polycrystalline (pc) Au wire (Engelhard, 99.99%) in a gas/air torch flame and allowing it to cool down in air at room temperature. The counter electrode was a large-area Au electrode of the same quality. A conventional hydrogen reference electrode (RHE) made

(1) Galindo, M. C.; Martins, M. E.; Arvia, A. J. *Anal. Asoc. Quim. Arg.* **1986**, *74*, 215.
(2) D'Agostino, A. T.; Ross, P. N., Jr. *J. Electroanal. Chem.* **1987**, *185*, 88.
(3) Perdriel, C. L.; Ipohorski, M.; Arvia, A. J. *J. Electroanal. Chem.* **1986**, *215*, 317.
(4) Chao, F.; Costa, M.; Tadjeddine, A. *Surf. Sci.* **1974**, *46*, 265.
(5) Dickermann, D.; Schultze, J. M.; Vetter, K. J. *J. Electroanal. Chem.* **1974**, *55*, 429.
(6) Sotto, M. *J. Electroanal. Chem.* **1976**, *69*, 229.
(7) Capon, A.; Parsons, R. *J. Electroanal. Chem.* **1972**, *39*, 275.
(8) Clavilier, J.; Nguyen Van Huong, Ch. *J. Electroanal. Chem.* **1977**, *80*, 102.
(9) Florit, M. I.; Martins, M. E.; Arvia, A. J. *J. Electroanal. Chem.* **1972**, *39*, 275.
(10) Angerstein-Koslowska, H.; Conway, B. E.; Barnett, B.; Mazota, J. *J. Electroanal. Chem.* **1979**, *100*, 417.
(11) Sotto, M. *J. Electroanal. Chem.* **1976**, *70*, 291.
(12) Cerviño, R. M.; Triaca, W. E.; Arvia, A. J. *J. Electroanal. Chem.* **1985**, *182*, 51.
(13) Canullo, J. C.; Triaca, W. E.; Arvia, A. J. *J. Electroanal. Chem.* **1984**, *175*, 337.
(14) Córdova Orellana, R.; Martins, M. E.; Arvia, A. J. *Electrochim. Acta* **1979**, *24*, 469.
(15) Córdova Orellana, R.; Martins, M. E.; Arvia, A. J. *J. Electrochem. Soc.* **1980**, *127*, 2628.
(16) Martins, M. E.; Podestá, J. J.; Arvia, A. J. *Electrochim. Acta* **1987**, *32*, 1013.
(17) Chao, F.; Costa, M. *C.R. Acad. Sci. Paris, Ser. C* **1977**, *284*, 603.
(18) Chao, F.; Costa, M.; El Kaim, P. *C.R. Acad. Sci. Paris, Ser. C* **1977**, *284*, 639.
(19) Chao, F.; Costa, M. *C.R. Acad. Sci. Paris, Ser. C* **1977**, *284*, 736.
(20) Chao, F.; Costa, M. Deuxième Congrès International L'Hydrogène dans Les Metaux, Paris, 1977.
(21) Chao, F.; Costa, M.; Parsons, R.; Grattepain, C. *J. Electroanal. Chem.* **1980**, *115*, 31.
(22) Hamelin, A. *J. Electroanal. Chem.* **1984**, *165*, 167.
(23) Hamelin, A.; Lipkowski, J. *J. Electroanal. Chem.* **1984**, *171*, 317.
(24) Vázquez, L.; Gómez Rodriguez, J. M.; Gómez Herrera, J.; Baró, A. M.; Garcia, N.; Canullo, J. C.; Arvia, A. J. *Surf. Sci.* **1984**, *181*, 98.

0743-7463/89/2405-0165$01.50/0

with a Pt foil under H_2 saturation at atmospheric pressure was employed. It was properly shielded to prevent possible diffusion of soluble Pt species to the working electrode compartment in the course of the experiments. This part of the experimental work comprised the following stages.

1. Electrode Pretreatment. The working electrode was firstly potential cycled in aqueous HF solution at 0.1 V/s, between −0.1 and 1.7 V, until the corresponding stabilized voltammogram was attained.

2. Electrochemical Faceting. The pretreated electrodes were subjected to repetitive square wave potential sweeps (RSWPS) during a certain time (τ), at a frequency (f) usually greater than 1 kHz between the lower (E_l) and the upper (E_u) potential limits. The operating parameters were changed in the following ranges: $-0.1\ V \leq E_l \leq 1.15\ V$, $1.00\ V \leq E_u \leq 1.7\ V$, $1\ kHz \leq f \leq 5\ kHz$, and $10\ min \leq \tau \leq 9\ h$. As far as the frequency is concerned, most runs were made at 2.42 kHz because at this value of f, independently of E_l and E_u, the largest effects could be noticed. A specific set of parameters is given in the Results section, for development of Au electrode surfaces of different electrochemical behaviors.

3. Voltammetric Characterization. Treated Au electrodes were characterized through conventional voltammetry in HF solutions at 0.1 V/s to follow the changes produced in the O electroadsorption/electrodesorption potential range. Surface changes were also followed through the stabilized voltammetric response for upd Pb, in 1 M $HClO_4$ + 10^{-3} M $Pb(ClO_4)_2$, at 0.02 V/s between −0.2 and 1.7 V. For this purpose, data reported for Au single-crystal electrodes under similar conditions[22,23] as for treated Au electrodes were taken as reference.

4. SEM Micrographs. The SEM micrographs were obtained in the conventional way by using a Phillips SEM PSM 500.

Potentiodynamic Aging Procedure. These runs were made with pc Au wire (Engelhard 99.99%) electrodes which were tested as follows.

1. Electrode Pretreatment. Each working electrode was firstly polished with alumina powder (Buehler 0.3 μm). Then, it was immersed for 1 min in a 1:1 H_2SO_4 + HNO_3 mixture, followed by repetitive rinsing with triply distilled water free of organic matter. Finally, the electrode was subjected to a potential cycling at 0.2 V/s between preset potential limits in the 1.59 V $\leq E_a \leq$ 1.74 V and −0.15 V $\leq E_c \leq$ −0.05 V ranges until the stabilized voltammogram was attained. Data on specific treatment conditions are indicated on the Results section.

2. Potentiodynamic Aging. It was performed in 1 M HF solution by applying a repetitive triangular potential sweep at 0.2 V/s between E_a and E'_c during the time τ (600 s $\leq \tau \leq$ 1800 s). The values of E_a were set in the potential range where the O electroadsorption/electrodesorption takes place, that is, between 1.59 and 1.74 V, and those of E'_c, between 0.99 and 1.19 V.

3. Changes Produced by the Potentiodynamic Aging. These changes were voltammetrically followed at 0.2 V/s in the same electrolyte, between the limits E_a and E_c already mentioned in paragraph 1. All experiments were made at 25 °C.

Results

Voltammetric and SEM Micrograph Changes Caused by RSWPS. As the surface changes of treated Au electrodes are followed through conventional voltammetry, it is necessary to refer briefly to the voltammetric features of the untreated Au electrode in 4 M HF. Thus, conventional voltammograms at 0.1 V/s of small spherical Au electrodes (Figure 1a) show peak O-I at 1.39 V and peak O-II at 1.48 V, both related to the O electroadsorption, and the single peak O–C at 1.14 V with a shoulder at its negative potential side associated with the O electrodesorption. Otherwise, the voltammetric response of upd Pb on untreated Au exhibits (Figure 1b) a pair of conjugated peaks at ca. −0.13 V (Pb-I), another pair of sharp peaks at −0.02 V (Pb-II), and a broad peak at ca. 0.26 V accompanied by a shoulder at 0.23 V (Pb-III). According to the literature,[22,23] peak Pb-I is related to Pb desorption from terraces whose width is less than four atoms, being more pronounced for two atoms, peak Pb-II corresponds to Pb desorption from terraces (111), and peak Pb-III is attributed to Pb stripping from (100) and (111) steps.

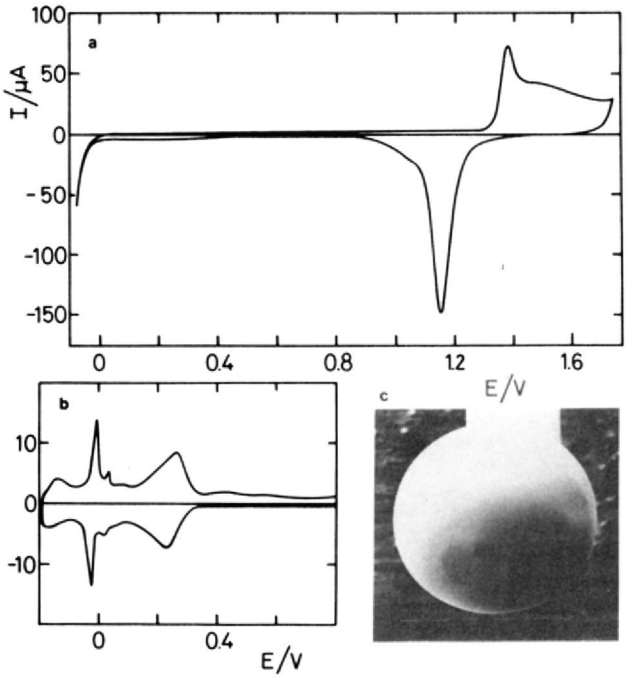

Figure 1. Untreated bead-shaped Au electrode. Apparent electrode area 0.024 cm². (a) Voltammogram run at 0.10 V/s in 4 M HF at 25 °C. (b) Voltammogram run at 0.02 V/s in 1 M $HClO_4$ + 10^{-3} M $Pb(ClO_4)_2$ at 25 °C. (c) SEM micrograph, scale 100 μm.

The SEM micrograph of the blank, that is, an Au electrode which has been potential cycled at 0.1 V/s in 4 M HF between −0.1 and 1.7 V during t = 4 h, shows the smooth topography which is typical of the preparation procedure (Figure 1c).

The result of the electrochemical faceting of Au, as for other metals,[12,13,24,25] depends mainly on the characteristics of the periodic perturbing potential, that is, f, E_l, and E_u, and to a less extent on the solution composition. It has been earlier[3,26,27] demonstrated that faceting of fcc metals such as Pt, Rh, Au, and Pd is principally caused by metal electrooxidation/electroreduction cycles (OCR) operating selectively as the perturbing potential moves at both sides of either the reversible potential of the metal/metal ion or the metal/metal oxide redox couples.

To study the onset potential for Au faceting in HF solutions and structure change, cyclic voltammograms of treated Au were successively investigated over a progressive range of E_u from 1.0 V upwards in 0.05-V increments by setting E_l = 0.50 V and f = 2.42 kHz for 1 h in 4 M HF. The onset potential for Au faceting is ca. 1.44 V. Therefore, only those electrodes treated for $E_u \geq 1.44$ V show voltammetric changes for upd Pb with respect to that of the blank (Figure 2). Thus, the RSWPS treatment applied for E_u = 1.44 V results in the decrease of the height of peak Pb-II, which in the reference system was assigned to Pb electrodesorption from (111) terraces. It also produces a considerable decrease in the contribution of the satellite peak located at the positive potential side of peak Pb-II, and the increase in the height of peak Pb-III, associated to Pb electrodesorption from (110) steps in the

(25) Custidiano, E.; Piovano, S.; Arvia, A. J.; Chialvo, A. C.; Ipohorski, M. *J. Electroanal. Chem.* **1987**, *221*, 229.
(26) Perdriel, C. L.; Triaca, W. E.; Arvia, A. J. *J. Electroanal. Chem.* **1986**, *205*, 279.
(27) Perdriel, C. L.; Custidiano, E.; Arvia, A. J. *J. Electroanal. Chem.* **1988**, *246*, 165.

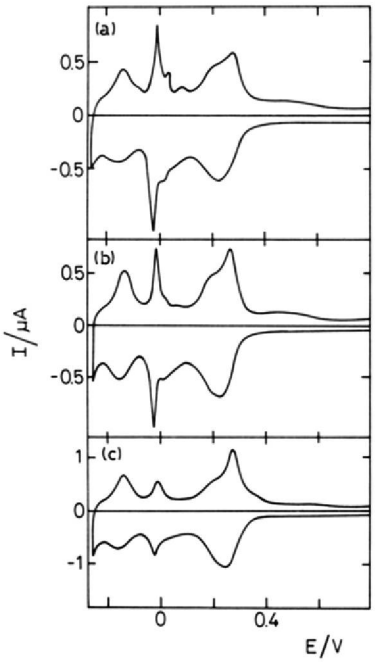

Figure 2. Bead-shaped Au electrode after 1 h of RSWPS in 4 M HF at f = 2.42 kHz and E_l = 0.50 V. Voltammograms run at 0.02 V/s in 10 M $Pb(ClO_4)_2$ + 1 M $HClO_4$. Apparent electrode area 0.025 cm^2. (a) E_u = 1.40 V. (b) E_u = 1.44 V. (c) E_u = 1.50 V.

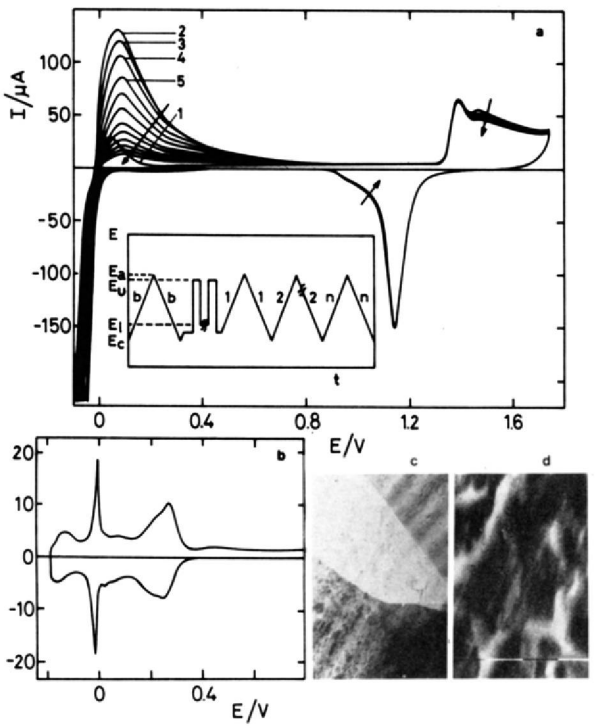

Figure 3. Bead-shaped Au electrode after 2 h of RSWPS in 4 M HF at f = 2.42 kHz, E_l = 1.1 V, and E_u = 1.60 V. Apparent electrode area 0.020 cm^2. (a) Voltammogram run at 0.10 V/s in 4 M HF at 25 °C; 1, 2, 3, 4, 5 denotes succesive cycles. (b) Voltammogram run at 0.02 V/s in 1 M $HClO_4$ + 10^{-3} M $Pb(ClO_4)_2$. (c) SEM micrograph, scale 100 μm. (d) SEM micrograph, scale 1 μm.

reference system. All these changes become even more remarkable for E_u = 1.50 V. The voltammetric response of these treated Au electrodes also exhibits an increase in the height of peak O-I.

Based on these results, the value of Eu was set at 1.6 V in order to study the influence of E_l. When E_l = 1.1 V, the voltammetric response of treated Au in 4 M HF shows

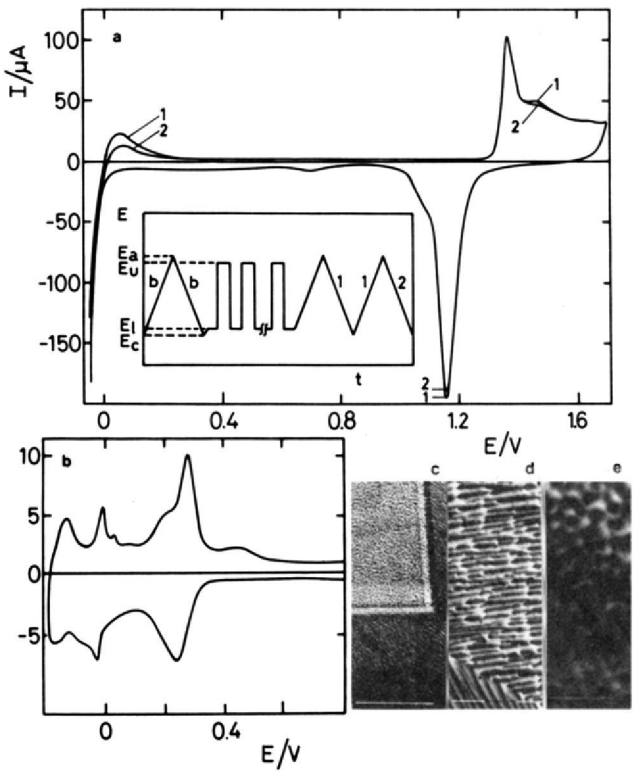

Figure 4. Bead-shaped Au electrode after 1 h of RSWPS in 4 M HF at f = 2.42 kHz, E_l = −0.1 V, and E_u = 1.60 V. Apparent electrode area of 0.027 cm^2. (a) Voltammogram run at 0.10 V/s and 4 M HF at 25 °C; 1 and 2 denote the first and second cycle, respectively. (b) Voltammogram run at 0.02 V/s in 1 M $HClO_4$ + 10^{-3} M $Pb(ClO_4)_2$. (c, d, e) SEM micrographs, scales 10, 1, and 1 μm, respectively.

an increase in both the charge of the O electroadsorption/electrodesorption region and the height of peak O-II. Accordingly, a clear enhancement of the HER current can be observed together with a broad anodic peak at 0.06 V (Figure 3a). The SEM micrographs show an irregular, inhomogeneous topography (Figure 3c). The voltammogram related to upd Pb on the treated Au electrode (Figure 3b) shows a well-defined sharp peak Pb-II, a shift of the potential of peak Pb-III positively at ca. 10 mV, and the corresponding shoulder better defined than that of the blank (Figure 1b). The comparison of these voltammograms to the reference system[22,23] suggests that preferred orientations in (111) and (110) directions have been accomplished through the RSWPS treatment under the conditions referred to above.

When the RSWPS treatment is made for f = 2.42 kHz, E_u = 1.60 V, and E_l = −0.1 V for 3 h (Figure 4a), the electrochemical behavior of the treated Au electrode surface exhibits a remarkable increase in the height of peak O-I and a substantial decrease in the HER activation. In this case, the increase in voltammetric charge produced by the electrochemical treatment as followed through the O electrodesorption charge is only about 10%. Correspondingly, SEM micrographs of the treated Au electrodes show an inhomogeneous electrochemical faceting with patches at the surface made of steps, others with an apparent porous structure, and finally regions with parallel porous-like channels (Figure 4c). Likewise, the voltammogram of upd Pb shows that the height of peak Pb-II decreases, whereas the heights of peaks Pb-I and Pb-III increase. These results in terms of the reference system can be interpreted as the development of (110) preferred orientation with a great density of steps and a little contribution of (111) terraces.

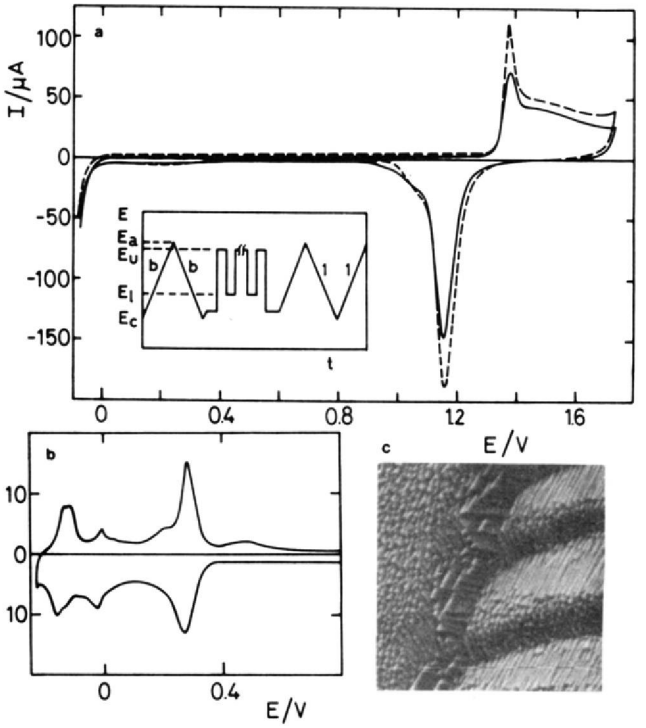

Figure 5. Bead-shaped Au electrode after 7 h of RSWPS in 4 M HF at f = 2.42 kHz, E_l = 0.50 V, and E_u = 1.60 V. (a) (---) Voltammogram run at 0.10 V/s in 4 M HF at 25 °C. (—) Untreated bead-shaped Au electrode. (b) Voltammogram run at 0.02 V/s in 1 M $HClO_4$ + 10^{-3} M $Pb(ClO_4)_2$. (c) SEM micrograph, scale 1 μm.

Finally, a clear electrochemical faceting results after a 1-h treatment for f = 2.42 kHz, E_u = 1.60 V, and E_l = 0.5 V. The corresponding voltammogram of upd Pb exhibits an enhancement of peaks Pb-I and Pb-III, which would be indicative of development of both (100) preferred orientation and steps.[22,23] Similar results are obtained for E_u = 1.7 V. Then, the voltammograms of treated Au electrodes show a net increase of peak O-I and a voltammetric charge increase of about 10% but without any appreciable change in activation for the HER (Figure 5a). Accordingly, the SEM micrographs show smooth and stepped regions inhomogeneously distributed. In this case the stepped surface regions show a clear faceting (Figure 5c).

Potentiodynamic Aging Data. Au Electrodes Activated for the HER. The voltammograms of Au electrodes run immediately after the potentiodynamic aging treatment described in the Experimental Section 2 (Figure 5a), in addition to the conventional peaks seen in the blank, exhibit a large increase in anodic and cathodic current between −0.2 to 0.2 V, that is, in the range of the HER, together with a new cathodic current extending from 1.0 to ca. 0.2 V. This cathodic current (dashed trace in Figure 6b), which corresponds largely to the electrodeposition of soluble Au species accumulated in the solution during the potentiodynamic aging treatment,[28] increases substantially as E_a is set more positive.

The increase in the HER current at E_c and υ = 0.2 V/s, after the potentiodynamic aging treatment ($I_{H_2}^{\tau}$) for τ = 900 s and E_a = 1.59 V, depends on E'_c. The greatest ($I_{H_2}^{\tau}/I_{H_2}^{0}$) ratio, where $I_{H_2}^{0}$ corresponds to the HER current read at E_c without potentiodynamic aging treatment (τ = 0), results in E'_c = 1.07 ± 0.03 V (Figure 7). Otherwise, for constant E'_c and τ, the $I_{H_2}^{\tau}/I_{H_2}^{0}$ current ratio increases

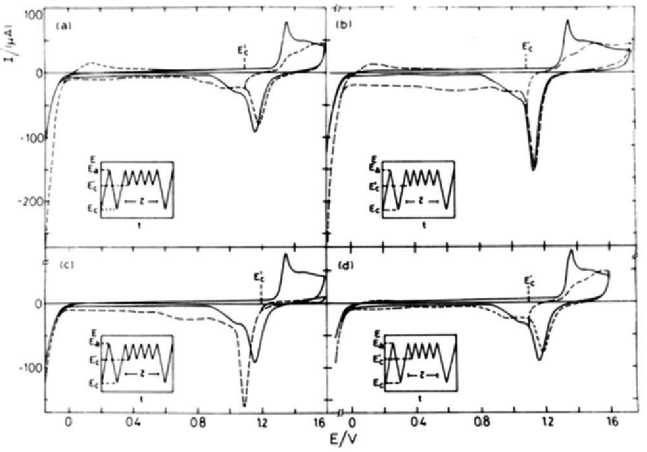

Figure 6. Voltammograms of Au electrodes run at 0.2 V s in 1 M HF at 25 °C (—) without activation and (---) after potentiodynamic aging perturbation, τ = 15 min. Apparent electrode area 0.24 cm^2. (a) E_c = −0.15 V, E'_c = 1.09 V, E_a = 1.59 V. (b) E_c = −0.15 V, E'_c = 1.09 V, E_a = 1.74 V. (c) E_c = −0.15 V, E'_c = 1.19 V, E_a = 1.59 V. (d) E_c = −0.10 V, E'_c = 1.10 V, E_a = 1.59 V.

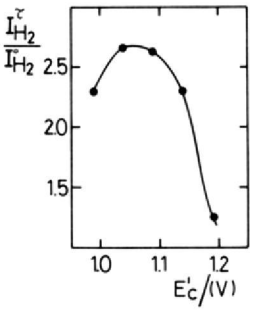

Figure 7. $I_{H_2}^{\tau}/I_{H_2}^{0}$ ratio vs E'_c. τ = 900 s, E_a = 1.59 V.

as E_a decreases, and for constant E'_c and E_a, it increases as τ increases. It should be noticed that the activation of the HER implies only a slight change in charge and position of peak O–C. Conversely, the features of this peak depend on whether E'_c is greater or lower than 1.19 V. Thus, for E'_c > 1.19 V an increase in height and charge of peak O–C can be observed, while its peak potential shifts negatively (Figure 6c) as E'_c is increased in the positive direction. For E'_c < 1.19 V, both the height and the charge of peak O-C decrease, and its peak potential moves positively as E'_c is increased stepwise (Figure 6a,b,d).

Discussion

The prolonged application of ORCs to Au electrodes in the potential range associated with the thermodynamic stability of bulk water, depending on the size and location of the potential window, can produce either electrochemical faceting, which is very remarkable for f > 1 kHz, or a transient activation for the HER for low f values, that is, $f \leq$ 0.4 kHz, υ = 0.2 V/s, E_a = 1.7 V, and E'_c = 1.09 V. Both effects, which result mainly from Au electrodissolution/electrodeposition cycles,[3,29-31] are more clearly seen in HF than in H_2SO_4 solutions.[3] Hence, the particular conditions associated with each one of those effects is primarily related to the relative position of E_u and E_l with respect to the reversible potential of the Au/Au(III) couple in HF solutions. This potential value which could not be found in the literature can be estimated as follows. The

(28) Folquer, M. E.; Zerbino, J. O.; de Tacconi, N. R.; Arvia, A. J. *J. Electrochem. Soc.* **1979**, *126*, 592.

(29) Cadle, S. H.; Bruckenstein, S. *Anal. Chem.* **1974**, *46*, 16.
(30) Rand, A. J. Woods, R. *J. Electroanal. Chem.* **1972**, *35*, 209.
(31) Sanftle, F. E.; Wright, D. S. *J. Electrochem. Soc.* **1985**, *132*, 129.

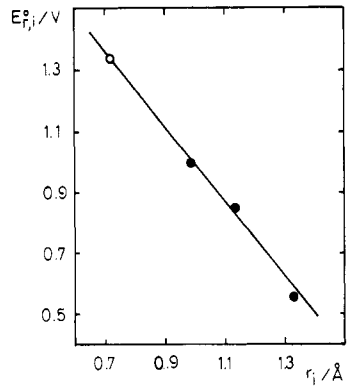

Figure 8. Dependence of the standard potential of the complex halide ions vs the covalent radii of the corresponding diatomic molecules: (●) values from literature; (○) extrapolated values.

electrodissolution of Au in HF solutions during the anodic half-cycle of ORC can be assigned to either one or both of the following overall reactions:

$$Au + 4F^- = AuF_4^- + 3e^- \quad (1)$$

$$Au + 2HF_2^- = AuF_4^- + 2H^+ + 3e^- \quad (2)$$

Equations 1 and 2 in turn depend on the following equilibria:

$$HF + H_2O = H_3O^+ + F^-; \quad K_1 = 7.2 \times 10^{-4} \quad (3)$$

$$F^- + HF = HF_2^-; \quad K_2 = 5.1 \quad (4)$$

The equilibrium potential ($E_{r,1}^\circ$) of reaction 1 was estimated by plotting the $E_{r,i}^\circ$ values of known reactions involving other complex halide ions out of fluoride ion vs the covalent radii (r_i) of the corresponding diatomic molecules (i). Thus, for the reactions[32]

$$AuCl_4^- + 3e^- = Au + 4Cl^-; \quad E_{r,5}^\circ = 1.00 \text{ V} \quad (5)$$

$$AuBr_4^- + 3e^- = Au + 4Br^-; \quad E_{r,6}^\circ = 0.85 \text{ V} \quad (6)$$

$$AuI_4^- + 3e^- = Au + 4I^-; \quad E_{r,7}^\circ = 0.56 \text{ V} \quad (7)$$

and $r_{Cl_2} = 0.99$ Å, $r_{Br_2} = 1.14$ Å, and $r_{I_2} = 1.33$ Å, the straight line plotted in Figure 8 was obtained, and by extrapolation of this line to $r_{F_2} = 0.72$ Å, the value $E_{r,1}^\circ = 1.34$ V is brought. When this figure is compared to the average periodic potential of the ORC, $\langle E \rangle = (E_a - E'_c)/2$, it results that only for values of $\langle E \rangle > 1.34$ V can net electrodissolution of Au in HF solutions be achieved. This is in agreement with the upper potential values required, for instance, for producing faceting effects. Likewise, under these circumstances the cathodic current assigned to the electrodeposition of soluble Au species can be voltammetrically detected over a relatively large potential range, including the *edl* region. In this case the cathodic current appears as various successive cathodic waves as expected for metal electrodeposition from different complex ions in solution.[33] The result of the cathodic reaction is the formation of an Au electrodeposited overlayer. The characteristics of the latter are determined also by the frequency of the periodic perturbing potential. At low frequencies, $f < 0.1$ kHz, when the HER activation effect prevails, there is evidence neither of faceting of the Au surface nor of aging effects for the O electroadsorbed layer, as no shift of the potential of the voltammetric peak O–C can be observed.[14-16] In this case, at low frequencies the Au overlayer results from the electrodeposition of soluble Au complex ions under diffusion control. Then, the thickness of the diffusional boundary layer as derived from the conventional voltammetric equation for soluble reactants[34] can be estimated on the order of 5×10^{-3} cm.

The nature of the resulting Au overlayer which exhibits activation properties for the HER can be ascribed to a thin Au layer of a few atoms thickness made of clusters presumably comparable to those resulting from the electroreduction of a relatively thick (about 100-nm thickness) hydrous Au oxide layer proceeding under either a slow linear potential sweep[35] or high negative potential steps.[36] In these last two cases the Au overlayer, according to ex situ scanning tunneling microscopy, is made of nearly spherical sticking metal clusters[37] which presumably can develop brushlike structures. The roughness of these structures depends on the amount of material which has been electroreduced.

On the other hand, at high frequencies, in the 1–10-kHz range, during each anodic half-cycle the electrochemical reaction supplies a high local concentration of soluble Au ions at the Au surface, provided that the duration of the anodic half-cycle allows the $Au(OH)_{ad}$ intermediate to undergo Au soluble species formation.[29,30,38] The kinetics of this reaction may be under either diffusion from the solution side or surface reaction control. The former case implies a concentration polarization, which diminishes as the average thickness of the pulsating diffusional boundary layer decreases, whereas the latter involves an activation polarization which is mainly determined by the exchange current density (j_0) values at each crystallographic face of the metal. For f values in the 1-kHz range the average thickness of the pulsating diffusion boundary layer results in the order of 10^{-5} cm. Hence, under these conditions the process is determined by the j_0 value of each crystallographic face.[39] Furthermore, in dealing with a surface reaction at pc Au one should also consider the specific work function of each crystallographic face,[40] that is, 5.11 eV for Au(111), 5.01 eV for Au(100), and 4.80 eV for Au(110). Therefore, in the absence of anion adsorption one should expect that the reactivity for Au electrooxidation decreases through the following sequence: (110) > (100) > (111). However, the specific adsorption of anions on Au[41,42] increases in the order (110) < (100) < (111), whereas the H_2O–Au interactions (hydrophilicity) decrease according to (110) > (100) > (111).[43] On the basis of these data one should expect that in concentrated HF solution, according to reactions 3 and 4, adsorbed HF_2^- ions initially predominate at Au(111) sites, that is, at the most densely packed atomic arrangement. This fact may change the reactivity for Au electrodissolution in the order (110) < (100) < (111)

(32) *Standard Potentials in Aqueous Solutions*; Bard, A. J., Parsons, R., Jordan, J. Eds.; Marcel Dekker: New York, 1985; pp 313, 318.
(33) *Encyclopedia of Electrochemistry of the Elements*; Bard, A. J., Ed.; Marcel Dekker: New York, 1975; Vol. IV, p 101.
(34) Levich, V. G. *Physicochemical Hydrodynamics*; Prentice Hall: Englewood Cliffs, NJ, 1962.
(35) Chialvo, A. C.; Triaca, W. E.; Arvia, A. J. *J. Electroanal. Chem.* **1984**, *171*, 303.
(36) Albano, E. V.; Martin, H. O.; Salvarezza, R. C.; Vela, M. E.; Arvia, A. J. unpublished results.
(37) Gómez, J.; Vázquez, L.; Baró, A. M.; Alonso, C.; González, E.; González-Velasco, J.; Arvia, A. J. *J. Electroanal. Chem.* **1988**, *240*, 77.
(38) Ferro, C. M.; Calandra, A. J.; Arvia, A. J. *J. Electroanal. Chem.* **1975**, *59*, 239.
(39) Visintin, A.; Canullo, J. C.; Triaca, W. E.; Arvia, A. J. *J. Electroanal. Chem.* **1988**, *239*, 67.
(40) Kirk, D. W.; Foulkes, F. R.; Graydon, W. F. *J. Electrochem. Soc.* **1981**, *127*, 1069.
(41) Bellier, J. P., Thèse de Doctorat d'Etat, Université Pierre et Marie Curie, Paris VI, 1980.
(42) Hamelin, A. *J. Electroanal. Chem.* **1983**, *144*, 365.
(43) Parsons, R. *J. Electroanal. Chem.* **1983**, *150*, 51.

provided that the ORCs promoted by the periodic perturbing potential are outside the time window related to the kinetics of anion adsorption. Therefore, when these conditions are fulfilled the Au surface resulting from the ORC treatment, at a frequency sufficiently high to overcome concentration polarization, appears to be principally related to the development of (110)-type preferred orientation accompanied by a slight increase in the electrode roughness.

Another possibility to develop electrochemical faceting of Au emerges when the fast ORC cycles, for instance, those covering between 1.1 and 1.6 V, allow a net accumulation of an Au oxide layer. In this case, the potential limits of the ORC can be compared to the equilibrium potential of the following redox processes:[32]

$$Au(OH) + H^+ + e^- = Au + H_2O; \quad E_{r,9}^\circ = 1.52 \text{ V} \quad (9)$$

$$AuO + 2H^+ + 2e^- = Au + H_2O; \quad E_{r,10}^\circ = 1.37 \text{ V} \quad (10)$$

$$Au(OH)_3 + 3H^+ + 3e^- = Au + 3H_2O; \quad E_{r,11}^\circ = 1.45 \text{ V} \quad (11)$$

Then, the Au surface resulting from the electroreduction at $E \ll E_1$ of the accumulated Au oxide layer appears to be related to a substantial development of (111)-type preferred crystallographic orientation including some roughness. The development of this type of preferred orientation at Au is comparable to that already described for Pt and Pd in acid solutions.[26,27]

In conclusion, depending on the characteristics of the periodic perturbing potential applied to Au electrodes in HF solutions, either activation for HER or different preferred crystallographic orientation can be achieved. The activation for the HER can be assigned to electrodissolution/electrodeposition of Au under diffusion control yielding a Au overlayer with transient activation properties for the adsorption and absorption of hydrogen.[14-16] The electrochemical faceting also implies electrooxidation and electrodeposition of Au occurring under surface reaction control. In this case it results in a major contribution of stepped surfaces with (110) preferred crystallographic orientation with some roughness. On the other hand, when the main process is the accumulation of a Au oxide layer and its subsequent electroreduction, the voltammetric response of the resulting surface exhibits a net HER activation effect. In this case the electrode surface becomes stepped with a trend to develop (111)-type preferred crystallographic orientation and roughness.

Acknowledgment. This work was supported by the Universidad Nacional de La Plata, the Consejo Nacional de Investigaciones Cientificas y Tēcnicas, and the Comisiōn de Investigaciones Cientificas (Provincia de Buenos Aires). This work is also partially supported by the Regional Program for the Scientific and Technological Development of the Organization of American States.

Registry No. Au, 7440-57-5; O_2, 7782-44-7; H_2, 1333-74-0; Pb, 7439-92-1; HF, 7664-39-3.

Interaction of Dimethyl Methylphosphonate with Metal Oxides

B. Aurian-Blajeni* and M. M. Boucher

EIC Laboratories, Inc., Norwood, Massachusetts 02062

Received April 4, 1988. In Final Form: August 25, 1988

Fourier transform infrared (FTIR) spectroscopy was used to investigate the gas–solid interactions of dimethyl methylphosphonate (DMMP) with metal oxide surfaces. The surface species is bound to the surface through the P=O bond. On titanium dioxide based powders, this bond could not be unambiguously seen. A correlation has been established between the labilization of the P=O bond by chemisorption and the electronegativity of the cations. The adsorption is a slow activated process.

Introduction

Some organophosphorus compounds are used as pesticides (e.g., *p*-nitrophenyl diethylphosphonate or Paraoxon) and warfare agents (e.g., isopropyl methylphosphonofluoridate or Sarin). The present study was prompted by the interest in means of decontamination of air and/or surface from organophosphorus compounds. We studied the behavior of dimethyl methylphosphonate (DMMP) as a simulant of such compounds.

DMMP can be decomposed by reaction with caustic reagents or by using the recently proposed micellar solution of *o*-iodosobenzoate as the decomposition catalyst.[1] There will still be cases in which water is undesirable (e.g., for decontamination of electronic devices). The catalytic decomposition of phosphorus compounds is an effective way of decomposition of DMMP, but it necessitates temperatures of 220 °C and more.[2] Decomposition of toxic vapor simulants is also possible by means of microwave irradiation.[2] It has been shown that particles of titanium dioxide and zinc in solution can be used to promote decomposition of phosphorus-containing compounds.[3] The remarkable stability of phosphorus compounds without aromatic substituents to electrochemical oxidation and reduction eliminates direct photoelectrochemistry as a

(1) Moss, R. A.; Kim, K. Y.; Swarup, S. *J. Am. Chem. Soc.* **1986**, 108, 788. Katritzky, A. R., Duell, B. L.; Durst, H. D. *Proceedings of the 1985 Scientific Conference on Chemical Defense Research*; Rausa, M., Ed., CRDEC-SP-86007, 1986; p 99. Hovanec, J. W.; Durst, H. D.; Ward, J. R. *Ibid.* p 111. Mackay, R. A.; Longo, F. R.; Knier, B. L.; Durst, H. D.; Burnside, B. A. *Ibid.* p 117.

(2) Bailin, L. J.; Sibert, M. E.; Jonas, L. A.; Bell, A. T. *Environ. Sci. Tech.* **1975**, *9*, 254.

(3) (a) Harada, K.; Hisanaga, T.; Tanaka, K. *New J. Chem.* **1987**, *11*, 597. (b) Rose, T. L.; Nanjundiah, C. *Proceedings of the 1985 Scientific Conference on Chemical Defense Research*; Rausa, M., Ed., CRDEC-SP-86007, 1986; p 299.

0743-7463/89/2405-0170$01.50/0